minerals

Article

Archean Zircons with Omphacite Inclusions from Eclogites of the Belomorian Province, Fennoscandian Shield: The First Finding

Oleg I. Volodichev, Oleg A. Maksimov *, Tatiana I. Kuzenko, Alexander I. Slabunov

Institute of Geology of the Karelian Research Center, Russian Academy of Sciences, Petrozavodsk 185910, Russia; volod@krc.karelia.ru (O.I.V.); tatianakuzenko8@gmail.com (T.I.K.); slabunov@krc.karelia.ru (A.I.S.)
* Correspondence olemaximov@mail.ru; Tel.: +79210115129

Abstract: Early Precambrian retrogressed eclogites are abundant in the central and northern parts of the Belomorian Province of the Fennoscandian Shield (Gridino + Keret and Salma + Kuru-Vaara study areas, respectively). Older and younger eclogites are recognized and their Archean and Paleoproterozoic ages are argued. Archean eclogites are intensely retrogressed and occur in amphibolite boudins in the tonalite-trondhjemite-granodiorite (TTG) gneiss matrix of the Archean Gridino eclogite-bearing mélange. Less retrogressed Paleoproterozoic eclogites form patches in mafic dikes and some amphibolite boudins; their Paleoproterozoic age is supported by U-Pb/SIMS data on zircons depleted in heavy rare earth elements (REE) with omphacite, garnet, and kyanite inclusions, and Sm-Nd and Lu-Hf mineral isochrons. Archean eclogites contain Archean heavy rare-earth elements (REE)-depleted zircons with garnet and zoisite inclusions and Archean garnets. No omphacite inclusions were found in these zircons, and this fact was considered as evidence against the existence of Archean eclogites. This study reports on the first finding of omphacite (23–25% *Jd*) inclusions in 2.68 Ga metamorphic zircons from eclogites from the Gridino eclogite-bearing mélange. The zircons are poorly enriched in heavy REE and display a weak negative Eu-anomaly but a poor positive Ce-anomaly typical of eclogitic zircons. Thus, zircons with these decisive features provide evidence for an Archean eclogite-facies metamorphism.

Keywords: Archean; eclogite; zircon; omphacite; geochronology; geochemistry; mineral inclusion; Gridino eclogite-bearing mélange; Belomorian province

Citation: Volodichev, O.I.; Maksimov, O.A.; Kuzenko, T.I.; Slabunov, A.I., Archean Zircons with Omphacite Inclusions from Eclogites of the Belomorian Province, Fennoscandian Shield: The First Finding. *Minerals* **2021**, *11*, 1029. https://doi.org/10.3390/min11101029

Academic Editor: José Francisco Molina

Received: 16 August 2021
Accepted: 19 September 2021
Published: 22 September 2021

1. Introduction

One of major problems to be resolved in modern geology is to answer the question: when did the present-day plate-tectonic processes, including subduction, begin on the Earth? [1–13]. One of the decisive indicators of convergent processes, such as subduction and collision, are crustal eclogites, mafic rocks that consist mainly of garnet and omphacite and formed at great depths at high (HP) and ultrahigh (UHP) pressures and relatively low temperatures. Therefore, finding the oldest eclogites may help to solve the above problem.

There are two regions in the world where eclogite-facies metamorphism of Archean age has been described: the Belomorian Province in the Fennoscandian Shield [14–17] and the Bundelkhand Craton in the Indian Shield [18]. However, many researchers believe that an Archean age of the oldest eclogites is not reliably proven [19] and that the oldest eclogites are Paleoproterozoic in age: 2.0 Ga in the Tanzanian Craton [20] and 1.9 Ga in the Atabasca Terrane in the Canadian Shield [21] and in the Belomorian Province of the Fennoscandian Shield [22–26].

The presence of Early Precambrian eclogites in the Belomorian Province is an undoubted fact (Figure 1a). These rocks are divided into two age groups, Archean and Paleoproterozoic, based on field observations and petrological and geochronological data [14,27–29]. Relics of the Archean eclogites have been recognized in boudins of amphibolites that along with their country tonalite-trondhjemite-granodiorite (TTG) gneisses build up the Archean Gridino eclogite-bearing mélange [15,30,31]. In the Archean eclogites zircons, depleted in heavy rare earth elements (REE) and containing inclusions of garnet and zoisite, have been described and Archean garnets have been recognized but no omphacite inclusions in Archean zircons have been revealed. The absence of omphacite inclusions is regarded as an argument of that Archean eclogites do not exist. Paleoproterozoic eclogites were derived after gabbroic rock dikes and locally make up boudins or their fragments [14,26,27,32–34]. The Paleoproterozoic age of these eclogites is reliably supported by heavy REE-depleted zircons with mineral inclusions of omphacite, garnet, and kyanite, as well as Sm-Nd and Lu-Hf mineral isochrons.

Thus, the prolonged discussion of the age of the Belomorian eclogites remains in progress [19,26,35,36]. It has recently been noted [37] that to finish the ongoing debate, Archean zircons, that in addition to their geochemistry characteristic of zircons from eclogites contain inclusions of eclogite-facies minerals, primarily omphacite and garnet, should be found [38,39]. This contribution deals with the first finding of Archean zircon with omphacite inclusions and new geochemical and geochronological data on zircons from retrogressed eclogites that occur in the well-studied eclogite body on Stolbikha Island in the Gridino eclogite-bearing mélange [14,22–25,27,29].

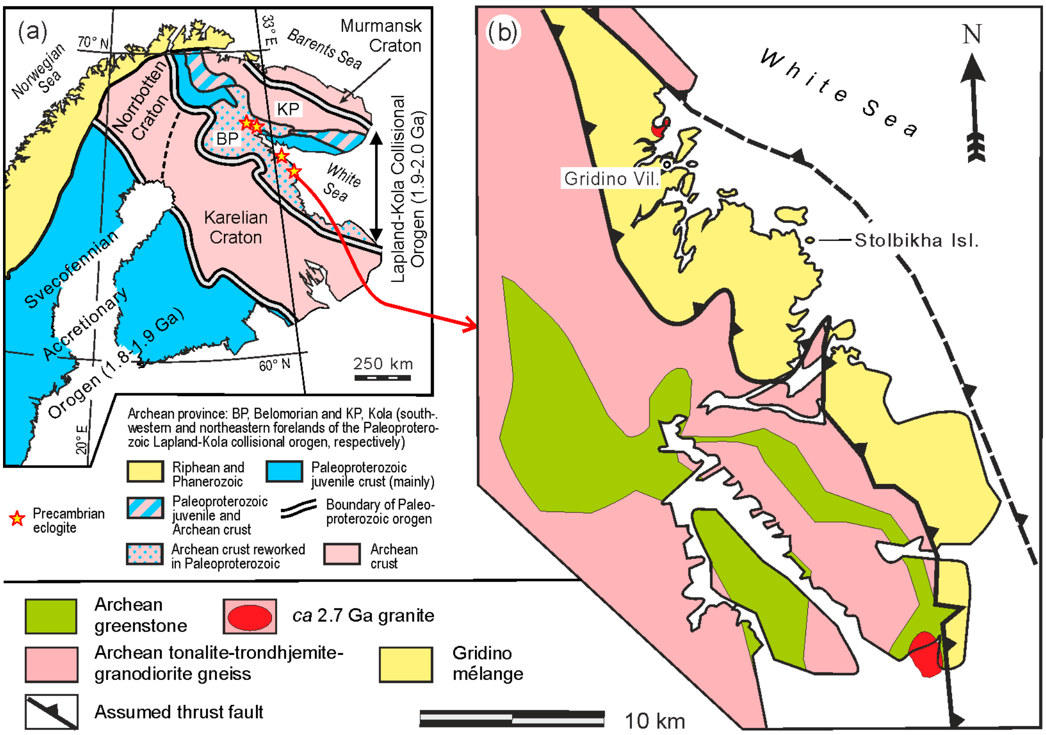

Figure 1. (**a**) Major tectonic units of the Fennoscandian Shield and location of Early Precambrian crustal eclogites (modified from [27]). (**b**) Geological sketch map of the Gridino study area showing the Gridino eclogite-bearing mélange (modified from [27]) and the location of Stolbikha Island where the studied eclogites are exposed.

2. Geological Setting

The eastern Fennoscandian Shield is mainly composed of Mesoarchean and subordinate Neoarchean rocks and was reworked during the Archaean Belomorian accretionary-collisional and Paleoproterozoic Lapland-Kola collisional orogenies (see review in [37]).

The Belomorian Province is built up by 2.9–2.6 Ga TTG gneisses, 2.9–2.7 Ga subordinate metavolcanics (including andesites, boninites), ultramafic rocks and metasediments and 2.9 Ga amphibolites with relics of eclogites [37,40], which compose nappes and tectonic sheets [17,29,35,37,40]. The Archean Belomorian and Paleoproterozoic Lapland-Kola orogenies are characterized by several deformational events under conditions of high- and moderate-pressure amphibolite- to granulite-facies metamorphism, which was locally superimposed on eclogites [14,17,22,25,27–29,35,37,41]. Eclogites that are assumed to be Archean in age occur as their almost completely retrogressed (symplectized) relics in Mesoarchean amphibolites hosted by TTG gneisses [15–17,27–29,37].

The earliest stage of the Archean tectonic evolution of the Belomorian Province is recorded by relics of ca. 2.9 Ga ophiolites that have been preserved in the Central Belomorian Mafite-Ultramafite Belt and an assumed ca. 3.0 Ga oceanic crust (hereafter, this Archean tectonic evolution is given after [37]). Three subduction stages and accretion cycles are supposed to have occurred at 2.88–2.82 Ga, 2.81–2.78 Ga, and 2.75–2.72 Ga. A northwest-trending subduction zone is marked by relics of eclogites [17,35] (Figure 1a) and the Central Belomorian Mafite-Ultramafite Belt whose constituent part is the Gridino eclogite-bearing mélange [17,35] (Figure 1b). Archean subduction is suggested to have occurred southwest- or northeast-wards and was followed by collision of the Archean Kola and Belomorian provinces and thrusting the former over the latter [17,35,37,40]. A collisional stage took place from 2.70 Ga to 2.66 Ga and includes elevated pressure amphibolite- to granulite-facies metamorphism), S-type leucogranites, volcanic molasse, potassic granites, and leucogabbros.

The main tectonic boundaries of the eastern Fennoscandian Shield were completely formed by the Paleoproterozoic Svecofennian accretionary and Lapland-Kola collisional orogenies, and the main tectonic unit of the northern and eastern parts of the shield is the Paleoproterozoic Lapland-Kola Collisional Orogen (LKO) [42,43]. The following stages of the tectonic development of the LKO are established: (i) intracontinental rifting of an Archaean crust (2.5–2.1 Ga); (ii) Red Sea-type oceanic separation between the Archean Belomorian and Kola provinces (2.1–1.97 Ga); (iii) subduction and crustal growth; the major structure composed of Paleoproterozoic juvenile crust is the Lapland Granulite Belt (1.97–1.90 Ga); (iv) intercontinental collision of the Belomorian Province against the Kola Province (1.94–1.86 Ga) [41,42]; and (v) orogenic collapse and exhumation (1.90–1.86 Ga) [42,44]. A south-westward subduction direction is assumed [45]; however, this needs further confirmation. Subduction and collision began in the eastern part of the LKO 10–30 Ga earlier than in the western part. The orogenic core is mainly composed of the Paleoproterozoic juvenile crust which makes tectonic sheets and nappes locally intercalated by sheets of the Archean crust (Figure 1a). The orogenic core is located between the Archean Kola north-east-verging and Archean Belomorian south-west-verging provinces interpreted as north-eastern and south-western forelands of the LKO, respectively [42,43]; the LKO possesses, thus, a palm-like structure [45]. Paleoproterozoic eclogites comprise patches of eclogitization superimposed on both Archean eclogites and early Paleoproterozoic mafic dikes and intrusions and differ in lower extent of retrogression [22–28,37]. These are suggested to have resulted from the Lapland-Kola collisional orogeny, which led tp high-pressure conditions in the lowermost parts of the over-thickened crust in the Belomorian Province [28] or from subduction of the Lapland-Kola oceanic crust [46].

The Archean Gridino eclogite-bearing mélange forms a large-scale tectonic sheet in the Gridino study area (Figure 1b) [40,41]. Its rocks display a more distinctive structure and composition than those of other complexes and tectonic units of the Belomorian Province. This tectonic sheet strikes northwestwards and can be traced for about 50 km in a 6–7 wide coastal strip and islands of the White Sea. The Gridino eclogite-bearing mélange is made up of repeatedly deformed and metamorphosed TTG gneisses that form the matrix and contain abundant boudins of amphibolites, often with relics of eclogites, as well as zoisitites and pyroxenites [14,40,46–48]. Six age groups of the Paleoproterozoic gabbroic dikes, dated at 2.50 Ga, 2.45 Ga, 2.40 Ga, 2.30 Ga, 2.23 Ga, and 2.12 Ga, are established in the Belomorian Province [49]. Four of them are recognized in the Gridino study area, cut the Gridino eclogite-bearing mélange [50], and 2.4 Ga, 2.3 Ga, and 2.12 Ga dikes display eclogitization [32,34,51].

A fragment of the Gridino eclogite-bearing mélange is well exposed on Stolbikha Island (Figure 2a). After the discovery of eclogites [14,52], this island has become a preserved natural site [53] and an object for scientific field trips [27,53–56]. Here, boudins consist of variably preserved eclogites, amphibolites, zoisitites, and pyroxenites.

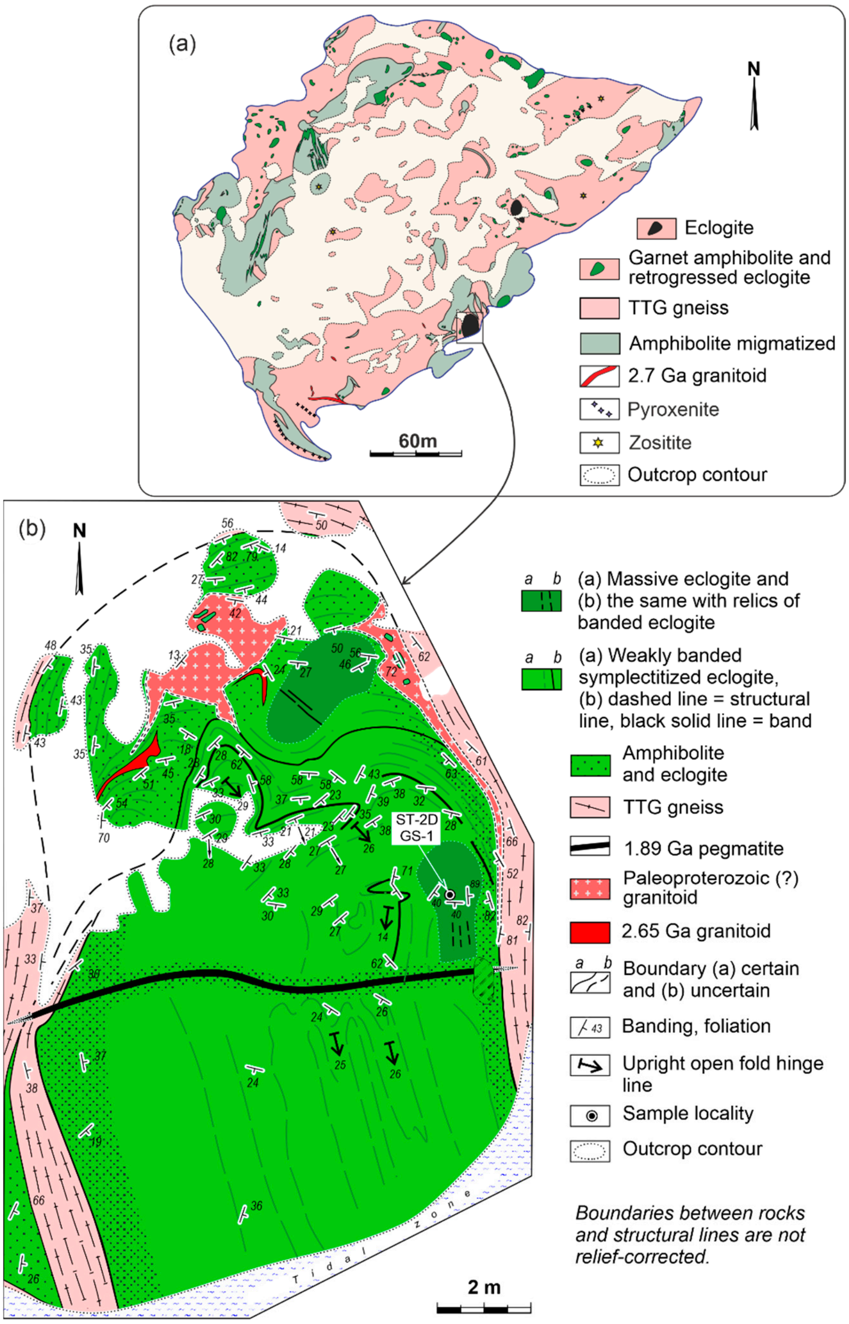

Figure 2. Geological maps of (**a**) Stolbikha Island and (**b**) an amphibolite boudin containing relics of eclogites (modified from [27]); samples from the massive eclogites: ST-2D (this study) and GS-1 [57].

The studied boudin of amphibolites with relics of eclogites occurs on the south shore of the island (Figure 2a). It is 9 m × 16 m in size (Figure 2b), has an oval contour on the surface and consists of: (i) banded intensely retrogressed eclogites deformed into isoclinal folds in central and western parts of the boudin, (ii) massive and weakly deformed eclogites in eastern and northern parts, and (iii) amphibolites, including garnet amphibolites, which evolved after eclogites at the boudin margins and along contacts of a pegmatite vein. The banded intensely retrogressed eclogites are cut by 2.65 Ga slightly sheared granitoids [27] and Paleoproterozoic (?) undeformed granitoids in the northern part of the boudin and by an 1890 ± 2 Ma [58] pegmatite vein in the central part (Figure 2b).

3. Petrological and Geochronological Outline

In the Gridino eclogite-bearing mélange, *P*–*T* conditions of eclogite-facies metamorphism are consistent with a pressure of 13–20 kbar and a temperature of 690–860 °C [14,27,46,47,57,59–63]. This wide range of *P* and *T* values also suggests that clastic constituent parts of the mélange (boudins) contain rocks formed at various depths [47,64]. The banded intensely retrogressed eclogites occur as an alternating 1–10 cm thick band of melanocratic and relatively leucocratic varieties. The melanocratic bands are typical symplectized eclogites with a diopside (*Di* with 6–8% jadeite = *Jd)*–plagioclase (*Pl* with 26–29% anortite = *An,* mineral abbreviations from [65]) symplectite matrix and conspicuous, compositionally homogeneous coarser garnet crystals (garnet = *Grt* with 21–23% pyrope = *Prp* and 24–25% grossular = *Grs*). One garnet grain contains an inclusion of omphacite (*Omp* with 23% *Jd*), indicating that eclogite-facies metamorphism occurred at a pressure of 14 kbar and a temperature of 750 °C [27,66]. Amphibole (*Amp*) is constantly present as a later mineral in the symplectite matrix.

The leucocratic bands display a more complex composition. They consist of symplectites (*Di* with 6–12% *Jd* and *Pl* with 26–32% *An*), whose integrated composition is consistent with a mixture of omphacite (20–28% *Jd* [66]) and garnet. Central domains of zoned garnets (*Grt* with 22–24% *Prp* and 28–32% *Grs*) contain abundant fine zoisite (*Zo*) and quartz (*Qtz*) inclusions. Calcic plagioclase (80–94% *An*) and diopside are present. A late mineral assemblage *Grt* + *Cpx* + *Amp* + *Bt* + *Pl* + *Qtz* formed under conditions of HP granulite facies (*P* = 11–14 kbar, *T* = 750–850 °C [27,66], *Cpx* = clinopyroxene, *Bt* = biotite).

The banded intensely retrogressed eclogites contain Archean zircons, which have been dated at 2721 ± 8 Ma, 2707 ± 31 Ma, and 2655 Ma [14,27,57] and bear inclusions of garnet [57] depleted in heavy REE [27,57]. The dominant garnet generation has an Archean age of 2.7 Ga (U-Pb, isotope dilution thermal ionization mass-spectrometry [67]). Available evidence suggests that the Archean zircons formed under eclogite-facies conditions, but some doubts still remain because mineral inclusions other than garnet and minerals indicative of eclogite-facies conditions (e.g., omphacite) have not been found in these zircons yet. It should also be noted that some Archean zircons have metamorphic rims, which are too thin for dating.

In spite of considerable multiple metamorphic retrogression, the massive eclogites are locally weakly retrogressed and display a well-preserved *Omp* + *Grt* assemblage (Figure 3, [14]). Garnets occurring in massive eclogites contain abundant inclusions of omphacite and amphibole, as well as intergrowths of these minerals. These garnets consist of 22–30% *Prp* and 18–29% *Grs* + andradite (*Adr)*; the average *Jd* content in omphacites is 23–25% at the maximum values of 31–33%. Central domains of complexly zoned crystals contain *Omp*, *Zo*, *Qtz*, and calcite (*Cal)* inclusions.

HP granulite-facies retrograde metamorphism of the massive eclogites is indicated by (i) a decline in the *Jd* content (13–18%) and the formation of numerous inclusions of *Pl* (20–22% *An*) and locally *Amp* in margins of *Omp* crystals; (ii) the formation of zones with abundant inclusions of *Cp*x (14–17% *Jd*), *Amp*, *Pl,* and *Cal* in garnets; (iii) the formation of coarse-grained symplectites S_1 (*Cpx* with 14–19% *Jd* and *Pl* with 19–24% *An*). Fine-grained symplectites S_2 (*Cpx* with 7–12% *Jd* and *Pl* with 22–24% *An*) also occur and indicate a subsequent retrograde stage under amphibolite-facies conditions. This retrograde process is better represented by an assemblage Grt (24% *Prp* and 27–28% *Grs*) + *Amp* + *Pl* (22–24% *An*) formed both in margins of complexly zoned garnets and in the matrix just near garnet crystals.

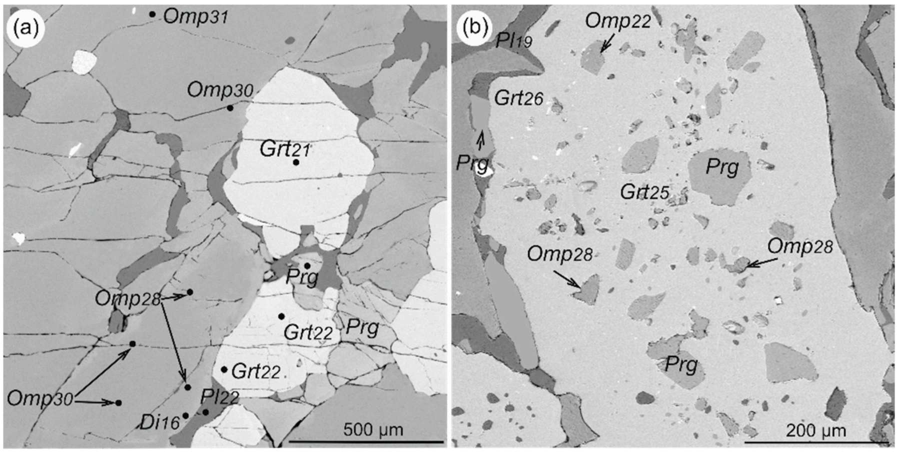

Figure 3. Back-scattered electron (BSE) images of thin sections of eclogites from the sampling site in the massive eclogite body: (**a**) best-preserved eclogite with minor retrogression, diopside (*Di*, subscript = *Jd* content) of a retrograde HP-granulite stage is located together with plagioclase (*Pl*, subscript = *An* content) and pargasite (*Prg*) in a narrow marginal zone of an omphacite (*Omp*, subscript = *Jd* content) crystal (thin section B-3 [14]); (**b**) garnet (*Grt* subscript = *Prp* content) crystal containing abundant inclusions of *Omp*, chlorine-bearing pargasite (*Prg*), and quartz (thin section from eclogite ST-2D).

The eclogite-bearing boudin also underwent later amphibolite-facies metamorphism. It is most conspicuous at its margins and along the 1.89 Ga pegmatite vein (Figure 2b). The margins are highly amphibolized and the marginal amphibolites look like amphibolites with relics of eclogite-facies mineral assemblages. Sample ST-2D that has been chosen for a geochronological study (Figure 2b) was taken from weakly amphibolized massive eclogite and contains only several domains in which a metamorphic reaction *Grt* + *Omp* + H_2O → *Amp* + *Pl* took place under decompression conditions.

In the massive eclogites, *P*–*T* conditions of eclogite-facies metamorphism and retrograde metamorphic stages were assessed by studying of contiguous crystal margins of coexisting minerals in accordance with the mineral equilibrium principle. Geothermometers [68–70] and geobarometers [71,72] were used. The following *P*–*T* parameters have been calculated: *P* = 13.7–14.1 kbar and *T* = 735–795 °C for the eclogite-facies metamorphism and *P* = 12.1–12.6 kbar and *T* = 750–765 °C for the subsequent HP granulite-facies retrograde event; *P* = 9.3–9.4 kbar and *T* = 670–675 °C for the later amphibolite-facies metamorphism, and *P* = 8.5 kbar and *T* = 650–660 °C for the amphibolite-facies metamorphic reworking that took place only in several domains. The initial stage of eclogite-facies metamorphism occurred at a pressure of 13 kbar and a temperature of 660 °C ([62], TWQ (Thermobarometry With Estimation of EQUilibrium state) method [73]) and the peak stage at a pressure of ~18.5 kbar and a temperature of 695–755 °C (pseudosection method [24,57]).

Later studies [22,24] suggested that (*i*) zircons from the massive eclogites consist of Archean presumably magmatic cores (2.75–2.70 Ga) and Paleoproterozoic metamorphic prismatic zircons (ca. 1.9 Ga [22]), some of which contain omphacite and garnet inclusions [24], and (ii) Paleoproterozoic eclogites formed after the protolith of Archean basic rocks. These suggestions are also supported by Lu-Hf mineral isochron ages of 1937 ± 8 and 1892 ± 10 Ma yielded by mineral assemblages with garnet [23].

4. Analytical Methods

A set of samples were cut out from the massive eclogites to select the most homogeneous and least retrogressed eclogites. Sample ST-2D was chosen as the most favorable for this purpose. Zircons were extracted from ~ 0.4 kg ST-2D sample using the "water-based" technique in a manner similar to that described in [74] for baddeleyite at the Laboratory of Matter Analysis, Institute of Geology of Ore Deposits, Petrography, Mineralogy, and Geochemistry from Russian Academy of Sciences (Moscow, Russia).

The geochronological study of zircons was carried out on a SHRIMP II ion microprobe at the Center for Isotope Research at the Karpinsky Russian Geological Institute (CIR VSEGEI), St. Petersburg, using a standard procedure [75,76]. Zircons were placed together with standard zircons 91500 [77] and Temora [78] into epoxy resin, polished to approximately half of the grains and coated with a ~100 Å thick 99.999% gold layer. The obtained results were processed using the program Isoplot/Ex version 4.15 (Berkeley Geochronological Center, Berkeley, CA, USA) [79] and decay constants from [80]. A correction for non-radiogenic lead was made based on the model described in [81] and the measured ratios $^{204}Pb/^{206}Pb$. The uncertainties in ages given in the work are reported at the 2 level.

The chemical composition of rock-forming minerals and micron-sized inclusions in zircons, as well as the internal structure of zircons, were analyzed on a VEGA II LSH (Tescan, Brno, Czech Republic) scanning electron microscope with an INCA Energy 350 energy dispersive detector at the Centre for Collective Usage, Karelian Research Centre from Russian Academy of Sciences (Petrozavodsk, Russia). The internal structure of zircons was also studied in cathodoluminescence at the CIR VSEGEI. Zircon trance-element composition (REE, Y, and Ti) was analyzed on a Cameca IMS-4f ion microprobe (Cameca, Gennevilliers, France) at the Yaroslavl Branch of the Valiev Institute of Physics and Technology from Russian Academy of Sciences (Yaroslavl, Russia). Chondrite-normalized compositions were used to construct REE patterns in zircons [82]. Zircon crystallization temperatures were determined with a Ti-in-zircon thermometer from [83].

5. Results

5.1. Zircon Morphology

The zircons extracted from massive eclogites were divided into three groups, based on their morphology and internal structure. The first group (Zrn-I) includes idiomorphic and sub-idiomorphic short-prismatic crystals up to 150 μm in size, which commonly display a mosaic and lesser sub-oscillatory internal structure in cathodoluminescence (CL). Some Zrn-I crystals consist of cores and later rims, and the latter have a distinctive light color in CL (Figure 4a). The second group (Zrn-II) comprises rounded crystals 40–60 μm in size with a complex internal structure which consists of very dark in CL cores and thin light in CL rims, and these constituent parts of Zrn-II crystals prominently differ from each other (Figure 4b). The third group (Zrn-III) embraces rounded grains 50–80 μm in size with a characteristic fir-tree and mosaic internal structure (Figure 4c). Characteristic features of Zrn-II are typical of those from granulite- and eclogite-facies metamorphic rocks [84–87].

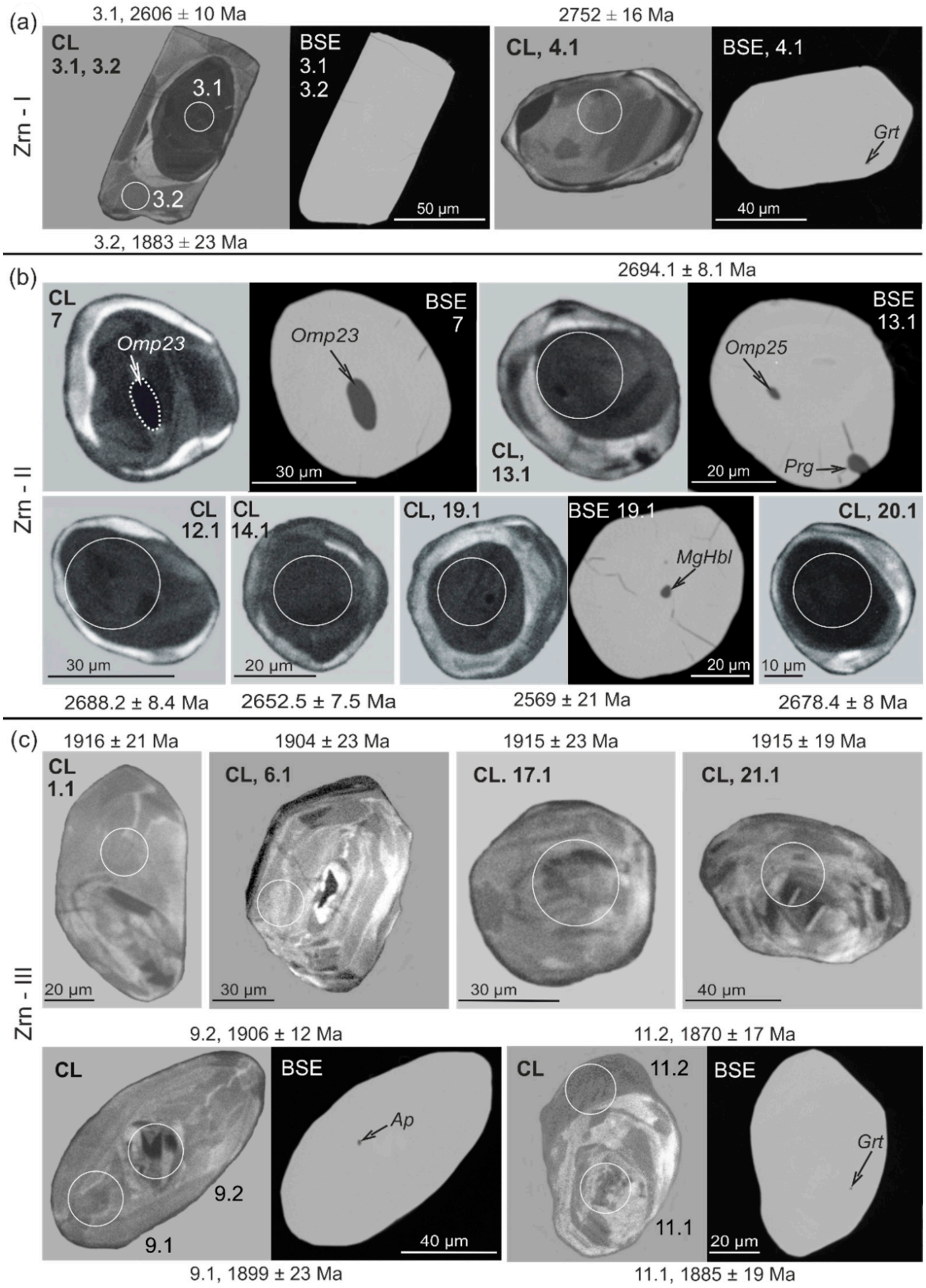

Figure 4. Cathodoluminescence (CL) and back-scattered electron (BSE) images of (**a–b**) Archean zircons Zrn-I (**a**) and Zrn-II (**b**), and Zrn-III (**c**) Paleoproterozoic zircons from eclogite ST-2D; ovals and circles indicate the SHRIMP spot locations (not to scale), and are labelled with the spot number and the approximate spot $^{207}Pb/^{206}Pb$ age (*Ap* = apatite).

5.2. Zircon Isotope Ages

Twenty-six U-Pb-Th isotope analyses were performed for the entire zircon population in sample ST-2D and these yielded both Archean and Paleoproterozoic $^{207}Pb/^{206}Pb$ ages. Fifteen analyses were made for Zrn-III crystals and age determinations fell into a range of 1.83 Ga to 1.93 Ga (Figure 5a) and yield a concordia age of 1895.5 ± 9.5 Ma. Nine crystals of Zrn-I and Zrn-II were dated and all of them were given Archean ages, which fell into a range of 2.65 Ga to 2.75 Ga (Figure 5a). One grain yielded a discordant age of 2405 ± 22 Ma (data-point 10.2, Table 1), which is considerably older than ages from Zrn-III crystals. Since its characteristic features considerably differ from those of Zrn-III crystals and are similar to those of Archean zircons, this grain is interpreted as an Archean one whose U-Pb-Th isotope system was strongly reset. Since this paper focuses on Archean zircons and their mineral inclusions, U-Th-Pb isotopic data are given only for Zrn-I and Zrn-II and are presented in Table 1 and Figure 5b,c.

One Zrn-I and five Zrn-II crystals have given concordant ages. The oldest concordant age of 2752 ± 32 Ma has been obtained for the only dated Zrn-I crystal (data-point 4.1, Table 1; Figures 4a and 5b). Four concordant and sub-concordant Zrn-II grains (data-points 5.1, 12.1, 13.1, and 20.1, Table 1) have yielded a concordia age of 2682 ± 9.4 Ma (Figure 5c) and a weighted average $^{207}Pb/^{206}Pb$ age of 2684.9 ± 8.5 Ma (Figure 5d). Thus, Zrn-II is rather confidently dated at 2.68 Ga, whereas the age of 2.75 Ga from the only dated crystal of Zrn-I can be accepted as tentative for the Zrn-I group and further dating is needed.

All Zrn-I and Zrn-II crystals display light in CL rims, which are usually 3–10 µm thick (Figure 4a,b) and only two rims were dated. These have given Paleoproterozoic ages: 1883 ± 46 Ma from a rim around a 2606 Ma Zrn-I crystal (Figure 4a) and 1885 ± 28 Ma from a rim around the 2405 Ma crystal with the strongly reset U-Th-Pb isotope system.

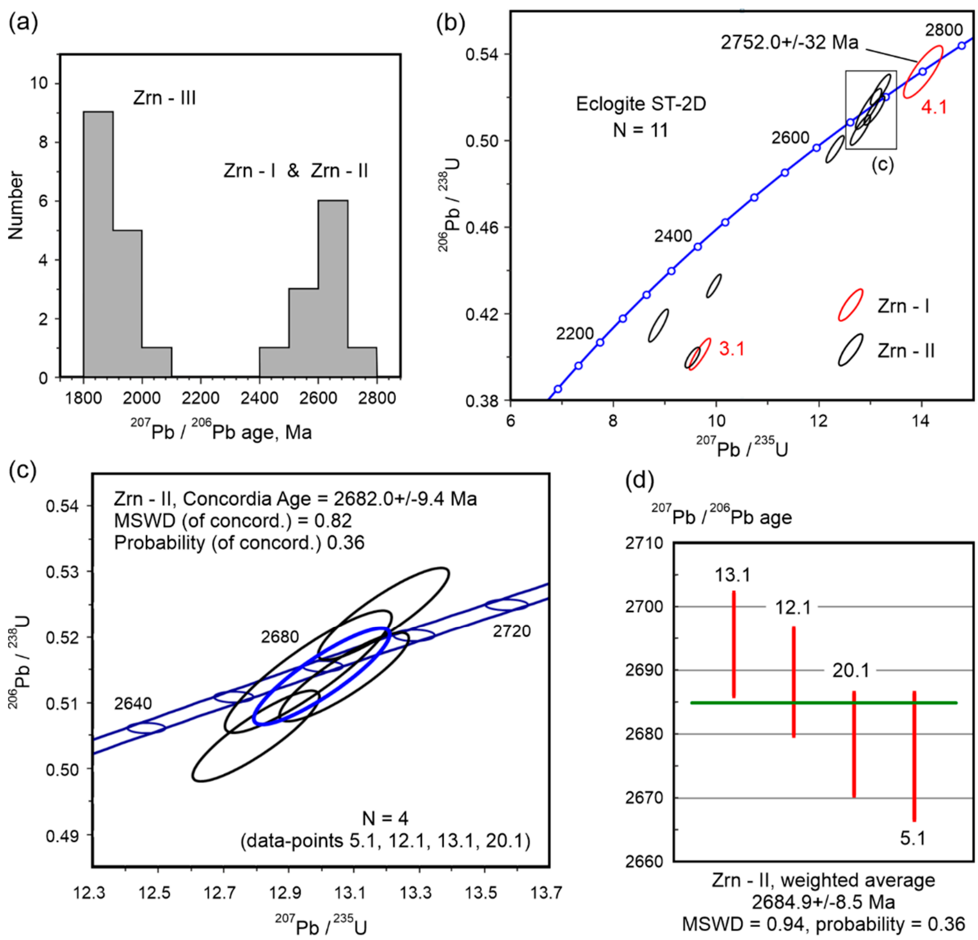

Figure 5. (**a**) Histogram, (**b**,**c**) concordia diagrams, and (**d**) weighted average $^{207}Pb/^{206}Pb$ age plot for zircons from eclogite ST-2D; data-point error ellipses and symbols are 68.3 % and 1σ confidence, respectively.

Table 1. U-Th-Pb isotope (SHRIMP-II) data for zircons from massive eclogite ST-2D.

Spot	$^{206}Pb_c$, %	U, ppm	Th, ppm	$^{232}Th/^{238}U$	$^{206}Pb^*$, ppm	Age, Ma (±1σ) $^{206}Pb/^{238}U$	Age, Ma (±1σ) $^{207}Pb/^{206}Pb$	D, %	$^{207}Pb^*/^{235}U$	±1σ, %	$^{206}Pb^*/^{238}U$	±1σ, %	$^{238}U/^{206}Pb^*$	±1σ, %	$^{207}Pb^*/^{206}Pb^*$	±1σ, %	Rho
Zrn-I group																	
3.1	0.20	203	20	0.10	70.2	2175 ± 22	2606 ± 10	20	9.68	1.4	0.4013	1.2	2.492	1.2	0.175	0.62	0.888
4.1	0.34	51	8	0.16	23.4	2749 ± 33	2752 ± 16	0	14.02	1.8	0.5319	1.5	1.88	1.5	0.1912	0.98	0.830
5.1	0.10	175	13	0.07	77.5	2677 ± 26	2676.5 ± 9.9	0	12.96	1.3	0.5147	1.2	1.943	1.2	0.1826	0.6	0.892
Zrn-II group																	
10.2	0.27	178	14	0.08	63.4	2236 ± 22	2405 ± 11	8	8.87	1.4	0.4145	1.2	2.412	1.2	0.1553	0.65	0.877
12.1	0.04	204	33	0.17	88.3	2635 ± 20	2688.2 ± 8.4	2	12.8	1	0.5049	0.9	1.98	0.9	0.18388	0.51	0.872
13.1	0.30	232	48	0.21	103	2673 ± 19	2694.1 ± 8.1	1	13.07	1	0.5139	0.87	1.946	0.87	0.18454	0.49	0.872
14.1	0.03	264	54	0.21	113	2597 ± 18	2652.5 ± 7.5	2	12.31	0.94	0.4961	0.82	2.016	0.82	0.17996	0.45	0.877
15.1	0.17	412	76	0.19	142	2167 ± 15	2588 ± 11	19	9.537	1	0.3996	0.79	2.503	0.79	0.1731	0.65	0.770
18.1	0.07	343	70	0.21	128	2318 ± 16	2524.7 ± 7.4	9	9.948	0.92	0.4328	0.8	2.31	0.8	0.16669	0.44	0.876
19.1	1.24	335	50	0.16	106	2004 ± 34	2569 ± 21	28	8.61	2.4	0.3647	2	2.742	2	0.1711	1.3	0.844
20.1	0.05	216	23	0.11	97.4	2714 ± 20	2678.4 ± 8	−1	13.19	1	0.5235	0.89	1.91	0.89	0.18279	0.48	0.880

Note: 1. Pbc, common lead corrected on the basis of measured ^{204}Pb. 2. Pb*, radiogenic lead. 3. D, discordance. 4. Rho, correlation coefficient of Pb/U ratios.

5.3. Zircon Geochemistry

In cores of 2.68 Ga Zrn-II grains, REE concentrations are 10 to 200 times higher than those in chondrite, display relatively smooth patterns, and show a slight enrichment in heavy REE: Lu_N/La_N = 14–169 and Lu_N/Gd_N = 1.06–15.68 (Table 2, Figure 6). Cores of Zrn-II grains display a mosaic internal structure typical for metamorphic zircons from high-grade rocks [86], and rounded morphology. In these zircons the Th/U ratio varies from 0.08 to 0.21 (Table 2). Generally, Th/U ratios of metamorphic and magmatic zircons are ≤ 0.1 and ≥ 0.5, respectively [88,89]. Thus, Th/U ratio values of ca, 0.1–0.5 are transitional between metamorphic and magmatic zircons and must be treated with caution [90,91]. Based on the mosaic structure of Zrn-II crystals, their metamorphic origin is more preferable. The most convincing feature of these zircons is inclusions of omphacite, a metamorphic mineral that forms under conditions of eclogite-facies metamorphism. All Zrn-II crystals display poor positive Ce and weak negative Eu anomalies (Figure 6) which also are typical of metamorphic zircons. Therefore, zircons of the Zrn-II group are metamorphic in origin.

Zircons of the Zrn-I group contain much lower U and Th concentrations than zircons Zrn-II; however, their Th/U ratios are identical to those from metamorphic Zrn-II crystals (0.07–0.16 and 0.08–0.21, respectively, Table 2). Compared with zircons of the Zrn-II group, the core of the 2.75 Ga Zrn-I crystal differs in the deepest negative Eu anomaly, though this anomaly itself is weak, and in the highest positive Ce anomaly (zircon 4.1, Table 2). Meanwhile, two other Zrn-I crystals (zircons 3.1 and 5.1, Table 2) exhibit REE patterns identical to those in 2.68 Ga metamorphic zircons Zrn-II, which suggest the same origin of Archean zircons Zrn-II.

The core of the 2.75 Ga Zrn-I crystal (zircon 4.1, Figure 4a) exhibits a well-defined mosaic internal structure that is characteristic of metamorphic zircons from granulite- and eclogite-facies rocks [86] and may be considered as metamorphic. This zircon core differs in much more differentiated REE concentrations, maximum Lu and minimum La concentrations, as well as the highest Lu_N/La_N (446) and Lu_N/Gd_N (68.3) and the lowest Sm_N/La_N (1.37) ratios. These values are typical of magmatic zircons and Zrn-I crystals could be identified as magmatic. However, light REE show differentiated patterns which coincide with those of zircons from samples taken from the massive eclogites [38], as well with those from Zrn-III of unambiguous metamorphic origin. Heavy REE display in turn patterns identical to those from Zrn-II crystals that are interpreted as metamorphic. The available data on the Zrn-I group do not permit to make a definitive conclusion on its origin. The metamorphic origin of these zircons is more preferable so far; however, further study is needed.

Patterns of chondrite-normalized REE concentrations in Paleoproterozoic zircons (Zrn-III) are shown in Figure 6, with Lu_N/La_N = 10.01–22.68, Lu_N/Gd_N = 1.15–2.00, and Sm_N/La_N = 1.88–5.46, and are consistent with those of zircons from eclogites in orogenic belts around the world [38] (Figure 6). These ratios are lower than those in Archean omphacite-bearing zircons (Zrn-II, Table 2, Figure 6).

The Ti-geothermometer [83] shows that the crystallization temperatures of Archean zircons vary from 701 °C to 775 °C (Table 2) and are similar to those of eclogite-facies metamorphism.

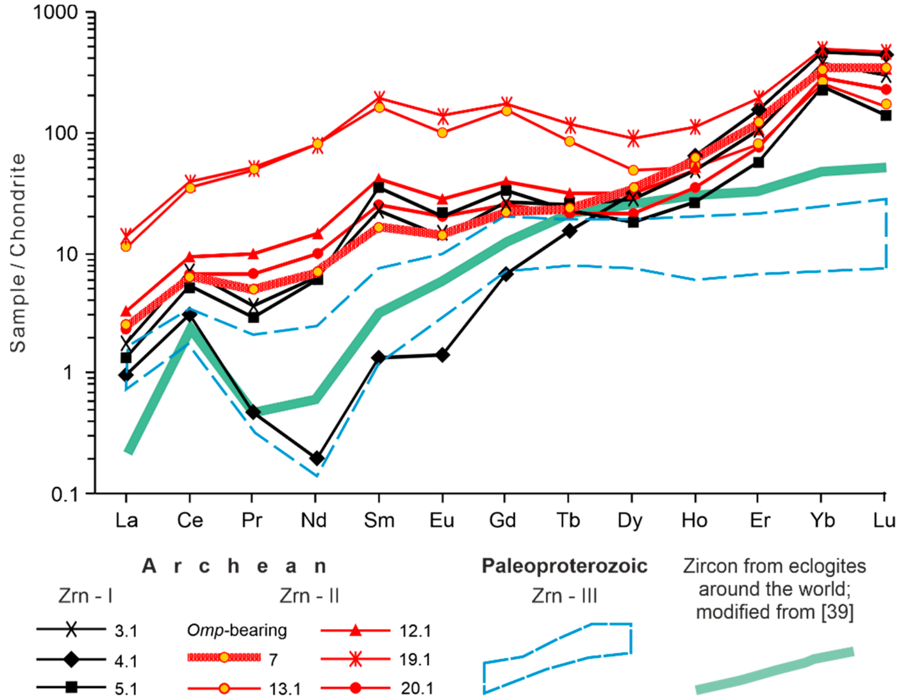

Figure 6. Chondrite-normalized [82] REE concentrations in zircons from eclogite ST-2D eclogites against those in zircons from eclogites from orogenic belts around the world [38].

Table 2. Trace element concentrations (ppm) and element ratios in and crystallization temperatures of zircons from massive eclogite ST-2D.

Zircon Group	Zrn–I			Zrn–II				
Spot	3.1	4.1	5.1	12.1	13.1	14.1	19.1	20.1
La	0.58	0.326	0.447	1.05	3.68	4.46	4.48	0.753
Ce	6.01	2.62	4.55	7.91	29.8	28.2	33.3	5.62
Pr	0.468	0.0614	0.381	1.28	6.40	7.11	6.74	0.859
Nd	3.88	0.125	3.80	8.94	49.8	50.3	49.5	6.23
Sm	4.61	0.276	7.20	8.41	33.7	38.3	38.2	5.06
Eu	1.07	0.112	1.57	2.19	7.58	9.95	10.3	1.55
Gd	7.34	1.79	9.19	10.9	42	43.2	48.4	6.86
Tb	1.23	0.755	1.13	1.55	4.06	4.61	5.71	1.05
Dy	9.72	10.8	6.19	10.5	16.3	21.3	29.6	7.42
Ho	3.69	4.96	2.07	3.80	3.96	5.60	8.40	2.69
Er	23.5	33.5	13	23.3	17.5	27.7	42.4	17.2
Yb	80.8	98.7	53.3	76.9	54.9	83.7	109	62.2
Lu	10.1	15	4.72	11	5.47	11.2	15.5	7.73
Y	118	168	68.3	121	126	185	251	91.9
Ti	10.3	7.75	8.40	7.83	14.6	7.69	185	6.21
Eu/Eu*	0.57	0.49	0.59	0.70	0.62	0.75	0.74	0.81
Ce/Ce*	2.76	4.43	2.64	1.63	1.47	1.20	1.45	1.67
∑REE	153.00	169.03	107.55	167.73	275.15	335.63	401.53	125.22
∑LREE	16.62	3.52	17.95	29.78	130.96	138.32	142.52	20.07
∑HREE	136.38	165.51	89.60	137.95	144.19	197.31	259.01	105.15
Lu_N/La_N	169.00	446.55	102.48	101.67	14.43	24.37	33.58	99.63
Lu_N/Gd_N	11.20	68.23	4.18	8.22	1.06	2.11	2.61	9.17
Sm_N/La_N	12.88	1.37	26.11	12.98	14.84	13.92	13.82	10.89
$^{207}Pb/^{206}Pb$ age, Ma	2606 ± 10	2752 ± 16	2676.5 ± 9.9	2688.2 ± 8.4	2694.1 ± 8.1	2652.5 ± 7.5	2569 ± 21	2678.4 ± 8
T, °C	743	719	726	720	775	718	1084	701

5.4. Mineral Inclusions

The central domain of a 2694 ± 16 Ma Zrn-II grain (data-point 13.1, Figure 4b) contains an omphacite inclusion with 25% *Jd* (Table 3), and its marginal zone carries an amphibole inclusion (*Prg*). The central part of a zircon crystal (grain 7, Figure 4b) is similar in composition, morphology, and geochemistry to the 2694 ± 16 Ma omphacite-bearing Zrn-II grain and also hosts an omphacite inclusion with 23% *Jd* (Table 3). On BSE images, these omphacite inclusions have clear and sharp contacts with their zircon host (Figure 4b). No fractures that form a radial system around the omphacite inclusions have been revealed, although the internal grain structure is well-defined on BSE images. Thus, these mineral inclusions are concluded to have formed together with their host, Archean zircons, and are not related to a later metamorphic overprint. In contrast, an inclusion of amphibole (*Prg*) that is located in a later overgrowth around the Zrn-II omphacite-bearing crystal is unambiguously related to a fracture (Figure 4b).

Mineral inclusions in the zircon analyzed are relatively scarce. In addition to the above omphacite and amphibole inclusions (*Prg*), pyrrhotite, pyroxene, calcite, and high-Mg hornblende (*Mg-Hbl*, zircon with data-point 19.1, Figure 4) inclusions have been identified in Archean zircons.

Table 3. Chemical composition (wt.%), formula units, and major component contents (%) of omphacite in inclusions in Zrn-II crystals from massive eclogite ST-2D.

Data-Point	7	13.1
SiO_2	53.15	55.28
Al_2O_3	8.00	6.56
FeO*	6.60	5.12
MgO	10.48	11.93
CaO	18.50	17.44
Na_2O	3.26	3.65
Total	99.99	99.98
O	6	6
Si	1.94	2.00
Al (IV)	0.06	0
Al (VI)	0.28	0.28
Fe^{3+}	0.01	0
Fe^{2+}	0.19	0.15
Mg	0.57	0.64
Ca	0.72	0.67
Na	0.23	0.26
cation sum	4.00	4.00
Mg#	0.74	0.81
Jadeite	23.0	25.4
Acmite	0	0
Augite	77.0	74.6

6. Discussion

This study has revealed that the massive eclogites from a boudin on Stolbikha Island contain three age groups of zircons: two Archean (Zrn-I and Zrn-II) and one Paleoproterozoic. The oldest Archean ages, 2752 ± 32 Ma (this study), 2734 ± 12 Ma [22], 2761 ± 73 Ma [57], and 2745 ± 3.2 Ma [24] were reported from both the banded, folded, and intensely retrogressed (completely symplectized) eclogites and the massive eclogites. All the authors assume the magmatic origin of these zircons, i.e., these zircon ages are suggested to reflect an age of eclogite protoliths. A similar age of 2745 ± 24 Ma has been obtained for zoisitites protoliths (presumably anorthositic in composition) which are thought to be related to eclogite protoliths [92]. In the northern Belomorian Province, protoliths of eclogites seem to show an older, late Mesoarchean age (ca. 2.9 Ga) [16,17]. However, the magmatic origin of the 2.75 Ga Zrn-I group is not finally proved, and the metamorphic origin is more preferable so far. Thus, ages of protoliths of the Belomorian eclogites fall in an interval 2.75–2.9 Ga.

The younger Archean generation of metamorphic zircons has been found in both the slightly retrogressed and weakly retrogressed massive and banded eclogites is dated at ca. 2.68 Ga (this study, [14,27,57]). Neoarchean zircons containing garnet inclusions were found in the massive eclogites; these were dated at 2689 ± 5 Ma and are slightly depleted in heavy REE (sample GS-1 [57]). These zircons are identical in age and are similar in their characteristics to Neoarchean zircons Zrn-II dated at 2684.9 ± 8.5 Ma that contain inclusions of omphacite. Thus, the massive eclogites contain 2689 ± 5 Ma zircons with garnet inclusions and 2684.9 ± 8.5 Ma zircons with omphacite inclusions, these zircons being identical to each other in some parameters and similar in others. This fact evidences that a Neoarchean ca. 2.69 Ga mineral assemblage *Omp* + *Grt* has been preserved in the massive eclogites. Therefore, we can conclude that the first eclogite-facies metamorphism occurred in the Neoarchean times.

The data presented here do not mean that the discussion about a Paleoproterozoic eclogite-facies metamorphism [35] is over but these allow us to reliably identify a Neoarchean eclogite-facies metamorphism, which has been proven on the basis of field observations, petrological, and geochronological [14,93] data, as well as on an analysis of the crustal evolution of the Belomorian Province [14–16,27,37]. The first finding of omphacite, a mineral indicative of eclogite-facies metamorphism, in Archean zircons is consistent with available geochronological data [14,57,93].

Finally, we can say that protoliths of eclogites discovered in amphibolite boudins in the Belomorian Province are ca. 2.9–2.75 Ga basic rocks that were metamorphosed to eclogites in a subduction zone 2.72–2.68 Ga ago. These eclogites were then intensely and repeatedly metamorphosed under granulite- to amphibolite-facies conditions upon subsequent Archean collision and exhumation [14,37] and the Paleoproterozoic Lapland-Kola collisional orogeny [37]. Metamorphic overprint under amphibolite- to granulite-facies conditions that occurred immediately after eclogite-facies metamorphism is a characteristic feature of Phanerozoic subduction zones and is related to later stages of subduction and subsequent collision and exhumation [94]. According to our data on the studied massive eclogites, the Archean eclogite-facies metamorphism took place at P = 13.7–14.1 kbar and T = 735–795 °C, which are consistent with geothermal gradient of ca. 16.5 °C/km. Archean eclogites from other locality of the Gridino eclogite-bearing mélange underwent intense decompression in the Archean and were completely changed into *Di-Pl* symplectites at P = 12–14.5 kbar and T = 700–760 °C/km [95]. These P–T parameters are intermediate between high $\mathrm{d}T/\mathrm{d}P$ (amphibolite to granulite facies) and low $\mathrm{d}T/\mathrm{d}P$ (blueschist and eclogite facies) in Phanerozoic and several Proterozoic orogenic belts [19]. Thus, the Archean eclogite-facies metamorphism should have occurred at geothermal gradient lower than 16.5 °C/km and the Archean Belomorian eclogites can be classified as the lowest pressure eclogites. However, a body of petrological data on these rocks is very small so far and further study is needed.

The modern architecture of the Belomorian continental crust was mainly formed by the Archean Belomorian orogeny and can be adequately explained based on the present-day tectonics of lithospheric plates. A possible geodynamic scenario is discussed in [28,29,40] and needs to be considered in a more detailed study that should take into account the latest advances in regional and structural geology, metamorphic and magmatic petrology, mineralogy, and geochronology of the Belomorian Province. Some Belomorian eclogites also formed in the Paleoproterozoic [22,24,25,27,28,32,34,37] but a discussion of their formation is also beyond the scope of this paper.

7. Conclusions

This isotope-geochemical study of zircons from the Stolbikha massive eclogites in the Gridino eclogite-bearing mélange has shown that these rocks contain 2684.9 ± 8.5 Ma zircons with inclusions of omphacite (23–25% *Jd*). These Neoarchean zircons are identical in age and some geochemical parameters to 2689 ± 5 Ma rounded zircons from the same massive eclogites that are depleted or poorly enriched in heavy REE, display no negative Eu anomaly, show a poor positive Ce-anomaly, and bear garnet inclusions [57]. These features are typical of zircons formed under conditions of eclogite-facies metamorphism. Thus, this study, based on the first finding of Archean metamorphic zircons with omphacite inclusions and the literature data, provides evidence for an eclogite-facies metamorphic event that took place in the Belomorian Province 2685–2689 Ma ago. The eclogite-facies metamorphism is suggested to have resulted from a southwest-directed subduction during the Belomorian accretionary-collisional orogeny, which can be adequately explained from point of view of present-day plate tectonics.

Author Contributions: Conceptualization, O.I.V., O.A.M. and A.I.S.; methodology, O.I.V.; validation, O.I.V.., O.A.M., and A.I.S; investigation, O.I.V., O.A.M.; resources, O.I.V.; data curation, T.I. K., O.A. M.; writing—original draft preparation, O.I.V., O.A.M., and A.I.S.; writing—review and editing, O.I.V., O.A.M., and A.I.S.; visualization, T.I.K., O.A.M., and A.I.S.; supervision, A.I.S.; project administration, O.A.M. and A.I.S.; funding acquisition, O.I.V., O.A.M., and A.I.S. All authors have read and agreed to the published version of the manuscript.

Funding: This research was funded by state assignment to Institute of Geology Karelian Research Centre RAS AAAA-A18-118020290085-4.

Acknowledgments: The authors are thankful to Xiaoli Li for additional information on the location of sample GS-1. A.I.S. thanks International Geoscience Programme project 509 for interest to this researches. Victor V. Balagansky is highly appreciated for helping with the fieldwork, sampling of the massive eclogites, and constructive notes on the manuscript.

Conflicts of Interest: The authors declare no conflict of interest.

References

1. de Wit, M.J. On Archean granites, greenstones, cratons and tectonics: Does the evidence demand a verdict? *Precambrian Res*. **1998**, *91*, 181–226.
2. Griffin, W.L.; O'Reilly, S.Y.; Abe, N.; Aulbach, S.; Davies, R.M.; Pearson, N.J.; Doyle, B.J.; Kivi, K. The origin and evolution of Archean lithospheric mantle. *Precambrian Res*. **2003**, *127*, 19–41.
3. Rozen, O.M.; Shchipansky, A.A.; Turkina, O.M. *Geodynamics of the Early Earth: Evolution and Stability of Geological Processes*; Nauchyi Mir: Moscow, Russia, 2008; p. 184. (In Russian)
4. Davies, G.F. Gravitational depletion of the early Earth's upper mantle and the viability of early plate tectonics. *Earth Planet. Sci. Lett*. **2006**, *243*, 376–382.
5. Brown, M. Duality of thermal regimes is the distinctive characteristic of plate tectonics since the Neoarchean. *Geology* **2006**, *34*, 961–964.
6. Brown, M. Metamorphic Conditions in Orogenic Belts: A Record of Secular Change. *Int. Geol. Rev.* **2007**, *49*, 193–234.
7. O'Neill, C.; Lenardic, A.; Moresi, L.; Torsvik, T.H.; Lee, C.-T.A. Episodic Precambrian subduction. *Earth Planet. Sci. Lett*. **2007**, *262*, 552–562.
8. Condie, K.C.; Pease, V.V. *When Did Plate Tectonics Begin on Planet Earth?* Geological Society of America: Boulder, CO, USA, 2008; Volume 440, p. 294.
9. Shirey, S.B.; Richardson, S.H.; Harris, J.W. Mesoarchean to Mesoproterozoic Re-Os ages for sulfide inclusions in Orapa diamonds and implications for Kaapvaal-Zimbabwe craton development. In *9th International Kimberlite Conference. Extended Abstract*; IKZ: Frankfurt, Germany, 2008; 9IKC-A-00365.
10. van Hunen, J.; van den Berg, A. Plate tectonics on the early Earth: Limitations imposed by strength and buoyancy of subducted lithosphere. *Lithos* **2008**, *103*, 217–235.
11. Sizova, E.; Gerya, T.; Brown, M.; Perchuk, L.L. Subduction styles in the Precambrian: Insight from numerical experiments. *Lithos* **2010**, *116*, 209–229.
12. Dobretsov, N.L.; Turkina, O.M. Early Precambrian Earth history: Plate and plume tectonics and extraterrestrial controls. *Russ. Geol. Geophys.* **2015**, *56*, 978–995.
13. Windley, B.F.; Kusky, T.; Polat, A. Onset of plate tectonics by the Eoarchean. *Precambrian Res.* **2021**, *35*, 105980.

14. Volodichev, O.I.; Slabunov, A.I.; Bibikova, E.V.; Konilov, A.N.; Kuzenko, T.I. Archean eclogites in the Belomorian mobile belt, Baltic Shield. *Petrology* **2004**, *12*, 540–560.
15. Shchipansky, A.A.; Khodorevskaya, L.I.; Konilov, A.N.; Slabunov, A.I. Eclogites from the Belomorian Mobile Belt (Kola Peninsula): Geology and petrology. *Russ. Geol. Geophys.* **2012**, *53*, 1–21.
16. Shchipansky, A.A.; Khodorevskaya, L.I.; Slabunov, A.I. The geochemistry and isotopic age of eclogites from the Belomorian Belt (Kola Peninsula): Evidence for subducted Archean oceanic crust. *Russ. Geol. Geophys.* **2012**, *53*, 262–280.
17. Mints, M.V.; Belousova, E.A.; Konilov, A.N.; Natapov, L.M.; Shchipansky, A.A.; Griffin, W.L.; O'Reilly, S.Y.; Dokukina, K.A.; Kaulina, T.V. Mesoarchean subduction processes: 2.87 Ga eclogites from the Kola Peninsula, Russia. *Geology* **2010**, *38*, 739–742.
18. Saha, L.; Pant, N.C.; Pati, J.K.; Upadhyay, D.; Berndt, J.; Bhattacharya, A.; Satynarayanan, M. Neoarchean high-pressure margarite–phengitic muscovite–chlorite corona mantled corundum in quartz-free high-Mg, al phlogopite–chlorite schists from the Bundelkhand Craton, north Central India. *Contrib. Mineral. Petrol.* **2011**, *161*, 511–530.
19. Brown, M.; Johnson, T. Secular change in metamorphism and the onset of global plate tectonics. *Am. Mineral.* **2018**, *103*, 181–196.
20. Möller, A.; Appel, P.; Mezger, K.; Schenk, V. Evidence for a 2.0 Ga subductionzone: Eclogites in the Usagaran belt of Tanzania. *Geology* **1995**, *12*, 1067–1070.
21. Baldwin, J.A.; Bowring, S.A.; Williams, M.L.; Williams, I.S. Eclogites of the Snowbird Tectonic Zone: Petrological and U-Pb geochronological evidence for Paleoproterozoic high-pressure metamorphism in the western Canadian Shield. *Contrib. Mineral. Petrol.* **2004**, *147*, 528–548.
22. Skublov, S.G.; Astaf'ev, B.Y.; Marin, Y.B.; Berezin, A.V.; Mel'nik, A.E.; Presnyakov, S.L. New data on the age of eclogites from the Belomorian Mobile Belt at Gridino settlement area. *Dokl. Earth Sci.* **2011**, *439*, 1163–1170.
23. Herwartz, D.; Skublov, S.G.; Berezin, A.V.; Mel'nik, A.E. First Lu–Hf Garnet Ages of Eclogites from the Belomorian Mobile Belt (Baltic Shield, Russia). *Dokl. Earth Sci.* **2012**, *443*, 377–380.
24. Yu, H.L.; Zhang, L.F.; Wei, C.J.; Li, X.L.; Guo, J.H. Age and P-T Conditions of the Gridino eclogite in the Belomorian Province, Russia. *J. Metamorph. Geol.* **2017**, *35*, 855–869.
25. Yu, H.; Zhang, L.; Lanari, P.; Rubatto, D.; Li, X. Garnet Lu-Hf geochronology and P-T path of the Gridino-type eclogite in the Belomorian Province, Russia. *Lithos* **2019**, *326*, 313–326.
26. Melnik, A.E.; Skublov, S.G.; Rubatto, D.; Müller, D.; Li, X.-H.; Li, Q.-L.; Berezin, A.V.; Herwartz, D.; Machevariani, M.M. Garnet and zircon geochronology of the Paleoproterozoic Kuru-Vaara eclogites, northern Belomorian Province, Fennoscandian Shield. *Precambrian Res.* **2021**, *353*, 106014.
27. Balagansky, V.V.; Maksimov, O.A.; Gorbunov, I.A.; Kartushinskaya, T.V.; Mudruk, S.V.; Sidorov, M.Y.; Sibelev, O.S.; Volodichev, O.I.; Stepanova, A.V.; Stepanov, V.S.; et al. Archean and Paleoproterozoic eclogites and zoisitites in the Gridino area. In *Early Precambrian Eclogites of the Belomorian Province, Fennoscandian Shield. Field Guidebook*; Slabunov, A.I., Balagansky, V.V., Shchipansky, A.A., Eds.; KRC RAS: Petrozavodsk, Russia, 2019; pp. 11–48.
28. Babarina, I.I.; Sibelev, O.S. Deformation events in the Gridino zone, Belomorian Province, Fennoscandian Shield: Relationships between mafic dike swarms and eclogite-bearing mélange. *Int. Geol. Rev.* **2015**, *57*, 1605–1616.
29. Balagansky, V.; Shchipansky, A.; Slabunov, A.; Gorbunov, I.; Mudruk, S.; Sidorov, M.; Azimov, P.; Egorova, S.; Stepanova, A.; Voloshin, A. Archean Kuru-Vaara eclogites in the northern Belomorian Province, Fennoscandian Shield: Crustal architecture, timing and tectonic implications. *Int. Geol. Rev.* **2015**, *57*, 1543–1565.
30. Slabunov, A.I.; Burdyukh, E.V.; Babarina, I.I. Granulometry and spatial distribution of fragmented components of the Gridino eclogite-bearing mélange. *Geol. Miner. Karelia* **2007**, *10*, 27–34. (In Russian)
31. Sibelev, O.S. Gridino zone of mélange (Belomorian Mobile Belt): Geology and structure. *Geol. Miner. Karelia* **2012**, *15*, 28–37. (In Russian)
32. Volodichev, O.I.; Slabunov, A.I.; Sibelev, O.S.; Skublov, S.G.; Kuzenko, T.I. Geochronology, Mineral Inclusions, and Geochemistry of Zircons in Eclogitized Gabbronorites in the Gridino Area, Belomorian Province. *Geochem. Int.* **2012**, *50*, 657–670.
33. Kozlovskii, V.M.; Aranovich, L.Y. Petrology and thermobarometry of eclogite rocks in the Krasnaya Guba dike field, Belomorian Mobile Belt. *Petrology* **2010**, *18*, 27–49, doi:10.1134/S0869591110010029.
34. Berezin, A.V.; Travin, V.V.; Marin, Y.B.; Skublov, S.G.; Bogomolov, E.S. New U–Pb and Sm–Nd ages and P–T estimates for eclogitization in the Fe-Rich gabbro dyke in Gridino area (Belomorian Mobile Belt). *Dokl. Earth Sci.* **2012**, *444*, 760–765, doi:10.1134/S1028334X12060207.
35. Mints, M.V.; Dokukina, K.A. Age of eclogites formed by the subduction of the Mesoarchaean oceanic crust (Salma, Belomorian Eclogite Province, eastern Fennoscandian Shield, Russia): A synthesis. *Precambrian Res.* **2020**, *350*, 105879, doi:10.1016/j.precamres.2020.105879.
36. Mints, M.V.; Dokukina, K.A. Reply to comments from S.G. Skublov, A.V. Berezin, and L.I. Salimgaraeva on the article authored by M.V. Mints and K.A. Dokukina—The Belomorian eclogite province (Eastern Fennoscandian shield, Russia): Meso-Neoarchean or Late Paleoproterozoic? *Geodyn. Tectonophys.* **2021**, *12*, 662–667, doi.org/10.5800/GT-2021-12-3-0545.
37. Slabunov, A.I.; Balagansky, V.V.; Shchipansky, A.A. Mesoarchean to Paleoproterozoic crustal evolution of the Belomorian Province, Fennoscandian Shield, and the tectonic setting of eclogites. *Russ. Geol. Geophys.* **2021**, *62*, 525–546, doi:10.2113/RGG20204266.

38. Skublov, S.G.; Berezin, A.V.; Berezhnaya, N.G. General Relations in the Trace Element Composition of Zircons from Eclogites with Implications for the Age of Eclogites in the Belomorian Mobile Belt. *Petrology* **2012**, *20*, 427–449.
39. Rubatto, D. Zircon trace element geochemistry: Partitioning with garnet and the link between U–Pb ages and metamorphism. *Chem. Geol*. **2002**, *184*, 123–138.
40. Slabunov, A.I. *Geology and Geodynamics of the Archean Mobile Belts Exemplified on Belomorian Province of the Fennoscandian Shield*; KRC RAS: Petrozavodsk, Russian, 2008; p. 296. (In Russian)
41. Slabunov, A.I.; Lobach-Zhuchenko, S.B.; Bibikova, E.V.; Sorjonen-Ward, P.; Balagansky, V.V.; Volodichev, O.I.; Shchipansky, A.A.; Svetov, S.A.; Chekulaev, V.P.; Arestova, N.A.; et al. The Archaean nucleus of the Fennoscandian (Baltic) Shield. *Mem. Geol. Soc. Lond*. **2006**, *32*, 627–644.
42. Daly, J.S.; Balagansky, V.V.; Timmerman, M.J.; Whitehouse, M.J. The Lapland-Kola orogen: Palaeoproterozoic collision and accretion of the northern Fennoscandian lithosphere. *Mem. Geol. Soc. Lond*. **2006**, *32*, 579–598, doi:10.1144/GSL.MEM.2006.032.01.35.
43. Lahtinen, R.; Huhma, H. A revised geodynamic model for the Lapland-Kola Orogen. *Precambrian Res.* **2019**, *330*, 1–19, doi:10.1016/j.precamres.2019.04.022.
44. Hölttä, P.; Huhma, H.; Lahaye, Y.; Mänttäri, I.; Lukkari, S.; O'Brien, H. Paleoproterozoic metamorphism in the northern Fennoscandian Shield: Age constraints revealed by monazite. *Int. Geol. Rev.* **2020**, *62*, 360–387, doi:10.1080/00206814.2019.1611488.
45. Balagansky, V.V.; Gorbunov, I.A.; Mudruk, S.V. Palaeoproterozoic Lapland-Kola and Svecofennian orogens (Baltic shield). *Her. Kola Sci. Cent. RAS* **2016**, *3*, 5–11. (In Russian with English Abstract)
46. Volodichev, O.I.; Kuzenko, T.I.; Maksimov, O.A. Geology and petrology of zoisitites from the Gridino eclogite-bearing complex, Belomorian province, Fennoscandian shield. *Trans. KRC RAS. Precambrian. Geol. Ser.* **2020**, *10*, 26–48. (In Russian)
47. Morgunova, A.A.; Perchuk, A.L. Petrology of Precambrian metaultramafites of the Gridino high-pressure complex (Karelia). *Russ. Geol. Geophys.* **2012**, *53*, 131–146.
48. Maksimov, O.A. Metamorphic evolution of pyroxenites from the Gridino eclogite- bearing complex (Pryanishnaya Luda Island). *Vestn. MSTU* **2014**, *17*, 320–328. (In Russian)
49. Stepanova, A.; Stepanov, V.; Larionov, A.; Salnikova, E.; Samsonov, A.; Azimov, P.; Egorova, S.; Babarina, I.; Larionova, Y.; Sukhanova, M.; et al. Relicts of Paleoproterozoic LIPs in the Belomorian province, eastern Fennoscandian Shield: Barcode reconstruction for a deeply eroded collisional orogeny. In *Large Igneous Provinces and Their Plumbing Systems. Geological Society of London Special Publications*; Srivastava, R.K., Ernst, R.E., Buchan, K.L., De Kock, M., Eds.; Geological Society of London: London, UK, 2021; p. 518, doi:10.1144/SP518-2021-30.
50. Stepanov, V.S.; Stepanova, A.V. Early Paleoproterozoic metagabbroids of the Gridino village area (Belomorian mobile belt). *Geol. Miner. Karelia* **2006**, *9*, 57–71. (In Russian)
51. Slabunov, A.I.; Volodichev, O.I.; Skublov, S.G.; Berezin, A.V. Main Stages of the Formation of Paleoproterozoic Eclogitized Gabbro-Norite: Evidence from U–Pb (SHRIMP) Dating of Zircons and Study of Their Genesis. *Dokl. Earth Sci*. **2011**, *437*, 396–400.
52. Volodichev, O.I. *The Belomorian Complex of Karelia (Geology and Petrology)*; Nauka: Leningrad, Russia, 1990; p. 248.
53. Makarizhin, V.V.; Medvedev, P.V.; Richancik, D.V. *Geological Sites of Karelia*; KRC RAS: Petrozavodsk, Russia, 2006; p. 192. (In Russian)
54. Volodichev, O.I.; Slabunov, A.I.; Stepanov, V.S.; Sibelev, O.S.; Travin, V.V.; Stepanova, A.V.; Babarina, I.I. Archean and Paleoproterozoic eclogites and Paleoproterozoic druzites, Gridino area, White sea. In *Belomorian Mobile Belt and It's Analogues: Geology, Geochronology, Geodynamics and Metallogeny. Field Guidebook and Extended Abstracts*; KRC RAS: Petrozavodsk, Russia, 2005; pp. 60–80.
55. Slabunov, A.I.; Volodichev, O.I.; Stepanova, A.V.; Sibelev, O.S.; Stepanov, V.S.; Babarina, I.I. Archean eclogites and Paleoproterozoic eclogitized gabbroids, Gridino area, White Sea. In *Karelian Craton Transect (Finland, Russia): Precambrian Greenstone Belts, Ophiolites and Eclogites*; Peltonen, P., Hölttä, P., Slabunov, A., Eds.; 33 IGC, The Nordic Countries: Oslo, Norway, 2008; pp. 36–53.
56. Volodichev, O.I.; Slabunov, A.I.; Stepanova, A.V.; Stepanov, V.S.; Sibelev, O.S. Archean eclogites and Paleoproterozoic eclogitized gabbroids, Gridino area, White sea. In *Precambrian High-Grade Mobile Belts. Belomorian Mobile Belt in the Eastern Fennoscandian Shield. Field Guidebook*; KRC RAS: Petrozavodsk, Russia, 2014; pp. 7–32.
57. Li, X.L.; Zhang, L.F.; Wei, C.J.; Slabunov, A.I. Metamorphic PT path and zircon U-Pb dating of Archean eclogite association in Gridino complex, Belomorian province, Russia. *Precambrian Res.* **2015**, *268*, 74–96.
58. Skublov, S.G.; Berezin, A.V.; Li, X.-H.; Li, Q.-L.; Salimgaraeva, L.I.; Travin, V.V.; Rezvukhin, D.I. Zircons from a Pegmatite Cutting Eclogite (Gridino, Belomorian Mobile Belt): U-Pb-O and Trace Element Constraints on Eclogite Metamorphism and Fluid Activity. *Geosciences* **2020**, *10*, 197–217.
59. Dokukina, K.A.; Konilov, A.N. Metamorphic evolution of the Gridino mafic dyke swarm (Belomorian eclogite province, Russia). In *Ultrahigh-Pressure Metamorphism. 25 Years after the Discovery of Coesite and Diamond*; Dobrzhinetskaya, L., Cuthbert, S., Faryad, W., Wallis, S., Eds.; Elsevier: Amsterdam, The Netherlands, **2011**; pp. 579–621.
60. Dokukina, K.A.; Bayanova, T.B.; Kaulina, T.V.; Travin, A.V.; Mints, M.V.; Konilov, A.N.; Serov, P.A. The Belomorian eclogite province: Sequence of events and age of the igneous and metamorphic rocks of the Gridino association. *Russ. Geol. Geophys.* **2012**, *53*, 1023–1054, doi:10.1016/j.rgg.2012.08.006.

61. Volodichev, O.I.; Kuzenko, T.I. Prograde and petrograde trends in evoluyion of archean eclogites metamorphism and their geodynamic interpretation (Karelia, Gridino village area). *Proc. Russia Miner. Soc.* **2013**, *3*, 28–51. (In Russian)
62. Perchuk, A.L.; Morgunova, A.A. Variable P–T paths and HP-UHP metamorphism in a Precambrian terrane, Gridino, Russia: Petrological evidence and geodynamic implications. *Gondwana Res.* **2014**, *25*, 614–629.
63. Maksimov, O.A. Geology and petrology of eclogites in the Samylino area (Belomorian Province of the Fennoscandian Shield). *Trans. KRC RAS. Precambrian Geol. Ser.* **2019**, *2*, 88–94, doi:10.17076/geo958. (In Russian)
64. Volodichev, O.I. Evolution of metamorphic processes in the Belomorian mobile belt. In *Precambrian High-Grade Mobile Belts. Extendend Abstracts*; KRC RAS: Petrozavodsk, Russia, 2014; pp. 115–116.
65. Kretz, R. Symbols for rock-forming mineral. *Amer. Miner*. **1983**, *68*, 277–279.
66. Maksimov, O.A.; Slabunov, A.I.; Balagansky, V.V.; Volodichev, O.I. Archean eclogites from the Belomorian Province (examples from the Gridino area). In *Abstract Volume of the 13th International Eclogite Conference*; KRC RAS: Petrozavodsk, Russia, 2019; p. 54.
67. Kaulina, T.V.; Mitrofanov, F.P.; Apanasevich, E.A.; Zhavkov, V.A.; D'yakov, S.N.; Sherstennikova, O.G. U-Pb dating of garnet. In *New Data on Geology and Mineral Deposits of the Kola Peninsula*; Mitrofanov, F.P., Ed.; Kola Science Centre of the RAS: Apatity, Russia, 2005; pp. 60–64. (In Russian)
68. Powell, R. Regression diagnostics and robust regression in geothermometer/geobarometer calibration: The garnet-clinopyroxene geothermometer revised. *J. Metamorph. Geol*. **1985**, *3*, 231–243.
69. Wells, P.R.A. P-T conditions in the Moines of the Central Highlands, Scotland. *J. Geol. Soc. Lond.* **1979**, *136*, 663–671.
70. Blundy, J.D.; Holland, T.J.B. Calcic amphibole equilibria and a new amphibole-plagioclase geothermometer. *Contrib. Mineral. Petrol*. **1990**, *104*, 208–224.
71. Holland, T.J.B. The reaction albite = jadeite + quartz determined experimentally in the range 600–1200 °C. *Amer. Miner*. **1980**, *65*, 129–134.
72. Hollister, L.S.; Grissom, G.C.; Peters, E.K.; Stowell, H.H.; Sisson, V.B. Confirmation of the empirical correlation of Al in hornblende with pressure of solidification of calc-alkaline plutons. *Amer. Miner*. **1987**, *72*, 231–239.
73. Berman, R.G. Thermobarometry using multiequilibrium calculations: A new technique, with petrological applications. *Can. Mineral*. **1991**, *29*, 833–855.
74. Söderlund, U.; Johansson, L. A simple way to extract baddeleyite (ZrO2). *Geochem. Geophys. Geosyst*. **2002**, *3*, doi:101029/2001GC000212.
75. Williams, I.S. U-Th-Pb Geochronology by Ion Microprobe. In *Applications of Microanalytical Techniques to Understanding Mineralizing Processes. Reviews in Economic Geology*; McKibben, M.A., Shanks, W.C., III, Ridley, W.I., Eds.; Society of Economic Geologist: Denver, CO, USA, 1998; Volume 7, pp. 1–35.
76. Larionov, A.N.; Andreichev, V.A.; Gee, D.G. The Vendian alkaline igneous suite of northern Timan: Ion microprobe U-Pb zircon ages of gabbros and syenite. *Mem. Geol. Soc. Lon.* **2004**, *30*, 69–74.
77. Wiedenbeck, M.; Allé, P.; Corfu, F.; Griffin, W.L.; Meier, M.; Oberli, F.; von Quadt, A.; Roddick, J.C.; Spiegel, W. Three natural zircon standards for U-Th-Pb, Lu-Hf, trace element and REE analyses. *Geostand. Newslett*. **1995**, *19*, 1–23.
78. Black, L.P.; Kamo, S.L.; Allen, C.M.; Aleinikoff, J.N.; Davis, D.W.; Korsch, R.J.; Foudoulis, C. TEMORA 1: A new zircon standart for Phanerozoic U-Pb geochronology. *Chem. Geol.* **2003**, *200*, 155–170.
79. Ludwig, K.R. *User's Manual for Isoplot 3.75–4.15: A Geochronological Toolkit for Microsoft Excel*; Berkeley Geochronology Center Special Publication: Berkeley, CO, USA, 2012; p. 5.
80. Steiger, R.H.; Jäger, E. Subcommission on geochronology: Convention on the use of decay constants in geo- and cosmochronology. Earth Planet. *Sci. Lett.* **1977**, *36*, 359–362.
81. Stacey, J.S.; Kramers, J.D. Approximation of terrestrial lead isotope evolution by a two-stage model. Earth Planet. *Sci. Lett.* **1975**, *26*, 207–221.
82. Taylor, S.R.; McLennan, S.M. *The Continental Crust: Its Composition and Evolution*; Blackwell: Oxford, UK, 1985; p. 312.
83. Watson, E.B.; Wark, D.A.; Thomas, J.B. Crystallization thermometers for zircon and rutile. *Contr. Miner. Petrol*. **2006**, *151*, 413–433.
84. Masamichi, M.; Hi, T. Prediction of crystal structures of minerals under extremal conditions by methods of energy minimization. *J. Miner. Soc. Jpn.* **1983**, *16*, 217–221.
85. Bibikova, E.V. *Uranium-Lead Geochronology of Early Stages of the Evolution of the Ancient Shields*; Nauka: Moscow, Russia, 1989; p. 180.
86. Corfu, F.; Hanchar, J.M.; Hoskin, P.W.O.; Kinny, P. Atlas of zircon textures. *Rev. Mineral. Geochem.* **2003**, *53*, 469–500.
87. Liati, A.; Gebauer, D.; Fanning, C.M. Geochronological evolution of HP metamorphic rocks of the Adula nappe, Central Alps, in pre-Alpine and Alpine subduction cycles. *J. Geol. Soc.* **2009**, *166*, 797–810.
88. Hoskin, P.W.O.; Schaltegger, U. The Composition of Zircon and Igneous and Metamorphic Petrogenesis. *Rev. Mineral. Geochem.* **2003**, *53*, 27–62.
89. Rubatto, D. Zircon: The Metamorphic Mineral. *Rev. Mineral. Geochem*. **2017**, *83*, 261–295.
90. Harley, S.L.; Kelly, N.M. Zircon: Tiny but Timely. *Elements* **2007**, *3*, 13–18.
91. Kohn, M.J.; Kelly, N.M. Petrology and Geo chronology of Metamorphic Zircon. In *Microstructural Geochronology: Planetary Records Down to Atom Scale*; Moser, D.E., Corfu, F., Darling, J.R., Reddy, S.M., Tait, K., Eds.; AGU: Washington, DC, USA, 2018; Volume 232, pp. 35–61.

92. Slabunov, A.I.; Volodichev, O.I.; Li, X.; Maksimov, O.A. Archean zoisitites of the Gridino eclogite-bearing melange, Belomorian province of the Fennoscandian shield: Geology, U-Pb zircon ages and geodynamic setting. *Trans. KRC RAS* **2015**, *7*, 85–103. (In Russian)
93. Bibikova, E.V.; Slabunov, A.I.; Volodichev, O.I.; Kuzenko, T.I.; Konilov, A.N. Isotopic-geochemical characteristics of Archean eclogites and alumina gneisses from the Gridino zone of the tectonic mélange of the Belomorian mobile belt, Baltic Shield. In *The Use of Isotopic Geochronology for Solving Problems in Geodynamics and Ore Genesis*; Kozakov, I.K., Kotov, A.B., Eds.; IPGG RAS: Saint-Petersburg, Russia, 2003; pp. 68–71. (In Russian)
94. Faryad, S.W.; Cuthbert, S.J. High-temperature overprint in (U)HPM rocks exhumed from subduction zones; A product of isothermal decompression or a consequence of slab break-off (slab rollback)? *Earth-Scien. Rev.* **2020**, *202*, 103108.
95. Maksimov, O.A.; Balagansky, V.V.; Slabunov, A.I.; Larionov, A.N. Two high-pressure metamorphic events in Early Precambrian eclogites of the Gridino area (Belomorian Province of the Fennoscandian Shield): Petrology and geochronology. *Petrology* **2022**, *30*, in press.